DOI: 10.3901/CJME.2011.**.***, available online at www.cjmenet.com; www.cjmenet.com.cn

# Receptance Coupling for Tool Point Dynamics Prediction on Machine Tools

ZHANG Jun[1, 2, *], SCHMITZ Tony[2], ZHAO Wanhua[1], and LU Bingheng[1]

1 *State Key Laboratory for Manufacturing System Engineering, Xi'an Jiaotong University, Xi'an 710049, China*
2 *Department of Mechanical and Aerospace Engineering, University of Florida, Gainesville FL 32611, United States*

Received January 26, 2010; revised January 18, 2011; accepted, 2011; published electronically January, 2011

**Abstract:** Chatter has been a primary obstacle to the successful implementation of high speed machining. The frequency response function(FRF) of the tool point is crucial for identification of chatter free cutting conditions. In order to quickly acquire the FRF of the different components combinations of machine tool, the assembly of machine tool was always decomposed into several parts, where the fluted portion of tool, however, was always treated as a uniform beam, and the associated discrepancy was ignored. This paper presents a new method to predict the dynamic response of the machine-spindle-holder-tool assembly using the receptance coupling substructure analysis technique, where the assembly is divided into three parts: machine-spindle, holder and tool shank, and tool's fluted portion. Impact testing is used to measure the receptance of machine-spindle, the Timoshenko beam model is employed to analyze the dynamics of holder and tool shank, and the finite element method(FEM) is used to calculate the receptance of the tool's fluted portion. The approximation of the fluted portion cross section using an equivalent diameter is also addressed. All the individual receptances are coupled by using substructure method. The predicted assembly receptance is experimentally verified for three different tool overhang lengths. The results also show that the equivalent diameter beam model reaches an acceptable accuracy. The proposed approach is helpful to predict the tool point dynamics rapidly in industry.

**Key words:** receptance coupling, dynamics, endmill, chatter

## 1 Introduction

With the continual increase in aerospace and automobile manufacturing requirements, high material removal rates are demanded in high speed machining, which can be achieved by increasing the spindle speed or axial depth of cut. One limitation to increasing the allowable axial depth is regenerative chatter, which has motivated many investigations on the chatter analysis and associated avoidance methods[1–3]. The stability lobe diagram can be used to identify stable and unstable cutting zones by modeling the relationship between the chip width and spindle speed. However, knowledge of the tool-point dynamic response is required for developing a specific stability lobe diagram for each machine-spindle-holder-tool combination.

Impact testing is widely used in research and industry to identify the tool-point dynamics response. However, this often requires significant testing time when many spindle-holder-tool combinations are available. Therefore, methods to predict the tool-point dynamics offer a preferred alternative. SCHMITZ, et al[4–7], developed a method referred to as receptance coupling substructure analysis (RCSA), which can be used to predict the assembly dynamics of the machine-spindle-holder-tool. In RCSA, the tool-holder has previously been modeled by using Euler-Bernoulli or Timoshenko beam theory, where the fluted tool was approximated as a uniform cylindrical beam. For example, PARK, et al[8], ERTÜRK, et al[9], NAMAZI, et al[10], and FILIZ, et al[11], carried out research on tool dynamics based on the equivalent diameter beam using the RCSA method. The equivalent diameter was first proposed by KOPS, et al[12] and was based on the equivalent compliance and moment of inertia to simplify the calculation of the end mill deflection. KIVANC, et al[13], derived the equivalent diameter based on the inertia of the cross section of the flute. Although the previous research results showed good agreement between the predicted model containing an equivalent diameter beam and experimental measurements, there is no literature to make a comparison between experiments, a finite element solution for the tool's fluted portion and the approximate constant cross section solutions. Therefore, the discrepancy is unknown for us. On the other hand, it is also necessary to analyze the assembly dynamics based on the actual structure in order to obtain a more accurate result.

In this study, a three-dimensional model for the actual fluted portion of the tool was created by Pro/Engineering software, and finite element method was employed to

* Corresponding author. E-mail: junzhang@mail.xjtu.edu.cn
This project is supported by National Basic Research Program of China (973 Program, Grant No. 2009CB724407), National Natural Science Foundation of China (Grant No. 51005175), and Chinese Scholarship Council (University of Florida)

calculate its dynamics. An equivalent diameter beam approximating the fluted portion was also discussed in order to draw a comparison. The Timoshenko beam model was employed to determine the receptances of the tool shank and holder subassembly. These receptances were then coupled to the spindle-machine dynamics which were acquired by impact testing and inverse RCSA. Finally, the assembly dynamics were experimentally validated for three different tool overhang lengths.

## 2 RCSA Method for Tool-holder-spindle-machine Assembly

### 2.1 Background of receptance and RCSA

In this section, a brief review of the RCSA method is presented based on the previous literature[4–7]. For an assembly consisting of two rigidly connected components, or substructures, as shown in Fig. 1(a), the assembly receptance, or frequency response function, $\boldsymbol{G}_{ij}$, can be expressed as

$$\boldsymbol{G}_{ij}=\begin{pmatrix}\boldsymbol{H}_{ij} & \boldsymbol{L}_{ij}\\ \boldsymbol{N}_{ij} & \boldsymbol{P}_{ij}\end{pmatrix}=\begin{pmatrix}\dfrac{\boldsymbol{X}_i}{\boldsymbol{F}_j} & \dfrac{\boldsymbol{X}_i}{\boldsymbol{M}_j}\\ \dfrac{\boldsymbol{\Theta}_i}{\boldsymbol{F}_j} & \dfrac{\boldsymbol{\Theta}_i}{\boldsymbol{M}_j}\end{pmatrix}, \tag{1}$$

where $\boldsymbol{H}$, $\boldsymbol{L}$, $\boldsymbol{N}$, and $\boldsymbol{P}$ refer to the spatial receptance matrices of the assembly, $\boldsymbol{X}_i$ and $\boldsymbol{\Theta}_i$ are the assembly displacement and rotation at coordinate $i$, and $\boldsymbol{F}_j$ and $\boldsymbol{M}_j$ are the force and moment applied to the assembly at coordinate $j$. If coordinate $i$ is coincident with coordinate $j$, the receptance is referred as the direct receptance; otherwise, it is a cross receptance.

The substructure receptances, $\boldsymbol{R}_{ij}$, as shown in Fig. 1(b), are defined in Eq. (2)

$$\boldsymbol{R}_{ij}=\begin{pmatrix}\boldsymbol{h}_{ij} & \boldsymbol{l}_{ij}\\ \boldsymbol{n}_{ij} & \boldsymbol{p}_{ij}\end{pmatrix}=\begin{pmatrix}\dfrac{\boldsymbol{x}_i}{\boldsymbol{f}_j} & \dfrac{\boldsymbol{x}_i}{\boldsymbol{m}_j}\\ \dfrac{\boldsymbol{\theta}_i}{\boldsymbol{f}_j} & \dfrac{\boldsymbol{\theta}_i}{\boldsymbol{m}_j}\end{pmatrix}, \tag{2}$$

where $\boldsymbol{x}_i$ and $\boldsymbol{\theta}_i$ are the substructure displacement and rotation at coordinate $i$, and $\boldsymbol{f}_j$ and $\boldsymbol{m}_j$ are the force and moment applied to the substructure at coordinate $j$.

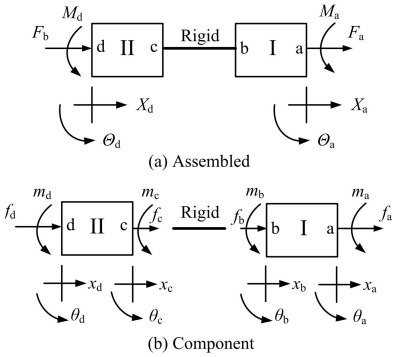


Fig. 1. Two components with a rigid connection

According to the coordinates identified in Fig. 1, the assembly direct receptances, $\boldsymbol{G}_{aa}$ and $\boldsymbol{G}_{dd}$, and the cross receptances, $\boldsymbol{G}_{ad}$ and $\boldsymbol{G}_{da}$ can be expressed as a function of the substructure receptances as shown in the following:

$$\boldsymbol{G}_{aa}=\boldsymbol{R}_{aa}-\boldsymbol{R}_{ab}(\boldsymbol{R}_{bb}+\boldsymbol{R}_{cc})^{-1}\boldsymbol{R}_{ba}, \tag{3}$$

$$\boldsymbol{G}_{dd}=\boldsymbol{R}_{dd}-\boldsymbol{R}_{dc}(\boldsymbol{R}_{bb}+\boldsymbol{R}_{cc})^{-1}\boldsymbol{R}_{cd}, \tag{4}$$

$$\boldsymbol{G}_{ad}=\boldsymbol{R}_{ab}(\boldsymbol{R}_{bb}+\boldsymbol{R}_{cc})^{-1}\boldsymbol{R}_{cd}, \tag{5}$$

$$\boldsymbol{G}_{da}=\boldsymbol{R}_{dc}(\boldsymbol{R}_{bb}+\boldsymbol{R}_{cc})^{-1}\boldsymbol{R}_{ba}. \tag{6}$$

### 2.2 Assembly receptance description

For a standard milling machine, the spindle section can be depicted as shown in Fig. 2 which identifies three individual components: the spindle-machine, holder and tool. Of these three, the dynamic response of the spindle-machine is most difficult to model due to its complicated structure and unknown damping behavior. Impact testing, therefore, is typically used to measure its dynamic behavior. The tool consists of a fluted portion and a constant shank portion; the holder's cross section is also constant over discrete intervals. The holder and shank portions are therefore convenient to model by Euler-Bernoulli or Timoshenko beam models. The fluted portion receptances can be calculated by the finite element method. In this work, the assembly is decomposed into three parts: the spindle-machine, the holder and tool shank and, finally, the tool's fluted portion, as shown in Fig. 3. After all components receptances obtained, the RCSA method can be applied to predict the assembly dynamics.

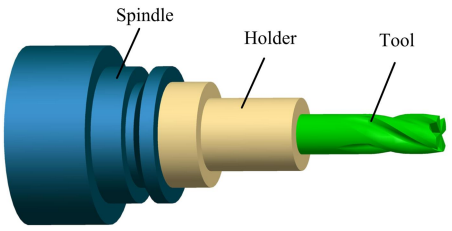


Fig. 2. Machine-spindle-holder-tool assembly

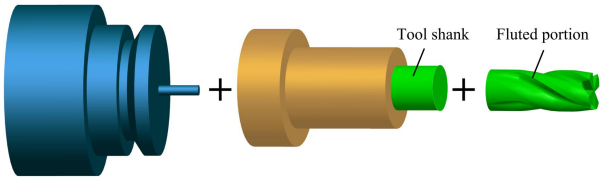


Fig. 3. Receptance coupling model of machine-spindle-holder-tool

## 3 Component Receptances Calculation

### 3.1 Fluted portion of the tool

Fig. 4 depicts the fluted portion of the tool as well as the grids and loads used to calculate the associated receptances. The outer diameter $d_o$ and length $l_f$ are 19.05 mm and 49.3 mm, respectively. The right side $AB$ is the tool's free end and the left side $CD$ where the fluted portion end and the tool shank begins. Force 1 ($\boldsymbol{f}_1$) and force 2 ($\boldsymbol{f}_2$) are applied at locations $A$ and $C$ while moment 1 ($\boldsymbol{m}_1$) and moment 2 ($\boldsymbol{m}_2$) are applied on the two side surfaces, respectively. The deflections at locations $B$ and $D$ can be calculated under the condition of individual loads.

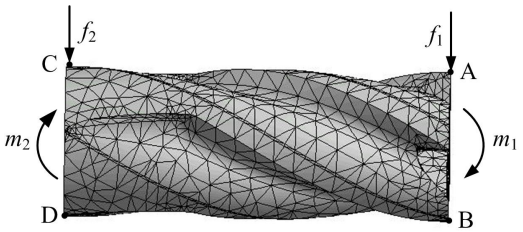


Fig. 4. Finite element model of fluted portion with loads

The finite element software ANSYS Workbench® 11.0 was used for calculations. The model was meshed by using 8 228 tetrahedral solid elements (Solid 187). From an investigation of the grid size on the results, little influence was found when using even finer grids. The material properties of the tool (carbide) were: Young's modulus $E$=550 GPa, Poisson's ratio $\nu$=0.22, density $\rho$=15 000 kg/m$^3$, damping ratio $\beta$=0.000 75. $\boldsymbol{f}_1$, $\boldsymbol{f}_2$, $\boldsymbol{m}_1$, and $\boldsymbol{m}_2$ were set to a value of 1 N (or N • m) and free boundary conditions were applied on the surfaces $AB$ and $CD$. Direct and cross receptances $\boldsymbol{R}_{ij}$ ($i$, $j$=1, 2) and the individual components listed in Table 1 were calculated according to the definitions in section 2.1.

**Table 1. Direct and cross receptances for the fluted portion**

| Load | Direct receptance | | Cross receptance | |
|---|---|---|---|---|
| $\boldsymbol{f}_1$ | $\boldsymbol{h}_{11}$ | $\boldsymbol{n}_{11}$ | $\boldsymbol{h}_{21}$ | $\boldsymbol{n}_{21}$ |
| $\boldsymbol{f}_2$ | $\boldsymbol{h}_{22}$ | $\boldsymbol{n}_{22}$ | $\boldsymbol{h}_{12}$ | $\boldsymbol{n}_{12}$ |
| $\boldsymbol{m}_1$ | $\boldsymbol{l}_{11}$ | $\boldsymbol{p}_{11}$ | $\boldsymbol{l}_{21}$ | $\boldsymbol{p}_{21}$ |
| $\boldsymbol{m}_2$ | $\boldsymbol{l}_{22}$ | $\boldsymbol{p}_{22}$ | $\boldsymbol{l}_{12}$ | $\boldsymbol{p}_{12}$ |

Fig. 5 shows the predicted receptance $\boldsymbol{h}_{11}$ of the fluted portion for a frequency range from 200 Hz to 2 000 Hz.

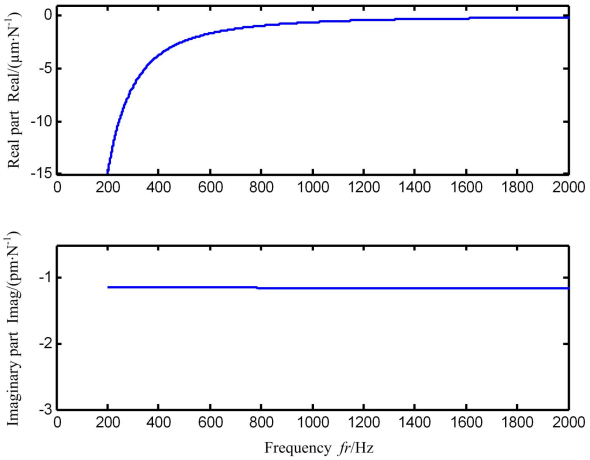


Fig. 5. Receptance $\boldsymbol{h}_{11}$ of the fluted portion of the tool

From Fig. 5, it is observed that no resonance occurred within this range. This is because the fluted portion is so short that the first natural frequency is much higher than 2 000 Hz, which is outside the measurement bandwidth of interest.

### 3.2 Equivalent diameter beam for the fluted portion

As described previously, finite element calculations were applied for the fluted portion, but this can be time-consuming for finely meshed models. As an alternative, an equivalent diameter of the fluted portion was also used to approximate the actual flute geometry[12–13]. For this study, the equivalent diameter was based on the principle of equivalent mass $m$. In this case, the equivalent diameter $d_{eq}$ can be calculated by

$$m = \rho\left[\frac{\pi}{4}(d_o^2(l_o + l_i) + d_{eq}^2 l_f\right], \tag{7}$$

where $l_o$ and $l_i$ are the overhang and inserted length of tool shank as shown in Fig. 6. Thus, the calculated $d_{eq}$ is 14.75 mm for the selected tool (shank diameter 19.05 mm).

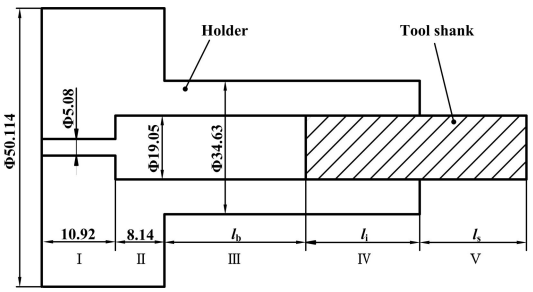


Fig. 6. Structure and dimensions of the holder and tool shank

The equivalent diameter uniform beam can be modeled as a Timoshenko beam, which is more accurate than the Euler-Bernoulli beam model because the former includes rotary inertia and shear effects. It is implemented using FEM[14]. Each four degree of freedom (rotation and displacement at both ends) free-free beam section was modeled by using appropriate mass ($\boldsymbol{M}$) and stiffness ($\boldsymbol{K}$)

matrices[15]. The element $\boldsymbol{M}$ and $\boldsymbol{K}$ matrices are then collected to form the global mass and stiffness matrices. Applying Guyan reduction[14], the equation of motion in the frequency domain can be obtained for $n$ elements. It can also be modeled as solid structure and solved by ANSYS Workbench® 11.0, similar to the fluted portion. Here, the receptances of the beam are defined as $\boldsymbol{R}_{ij}$ ($i$, $j$=3, 4).

Table 2 lists the two models' natural frequencies of the first three bending shape as well as the discrepancy of the equivalent diameter beam(EDB) model compared with actual fluted portion(AF) model. The largest error of this approximation method (EDB model) is 10.7%, which is seen for the first mode. From this table, it is seen that there is a very small discrepancy between FEM and Timoshenko beam solutions for the constant cross section EDB model.

**Table 2. Comparison of natural frequencies for the two models** Hz

| Mode | AF model | EDB model | |
|---|---|---|---|
| | FEM | FEM | Timoshenko |
| 1st | 29 386 | 32 516 (10.7%) | 32 524 (10.7%) |
| 2nd | 63 199 | 67 463 (6.7%) | 67 620 (7.0%) |
| 3rd | 97 645 | 104 080 (6.6%) | 104 900 (7.4%) |

### 3.3 Subassembly of the tool shank and holder

The holder and tool shank are both axisymmetric structure and can also be modeled as multi-segment Timoshenko beams. Fig. 6 shows the two dimensional structure and dimensions of the holder and tool shank. Considering different overhang lengths of the tool, three dimensions, tool shank overhang length $l_s$, tool length inserted in the holder $l_i$ and blank length of holder $l_b$ are provided in Table 3. The Timoshenko beam model for the structure was separated into five sections (I, II, III, IV and V) as shown in Fig. 6 and each section was modeled using 25 elements. The material properties of the holder were: $E$=200 GPa, $\nu$=0.29, $\rho$=7 850 kg/m$^3$, and $\beta$=0.000 75. The free-free tool shank and holder direct receptances $\boldsymbol{R}_{55}$ and $\boldsymbol{R}_{66}$, and the cross receptances $\boldsymbol{R}_{56}$ and $\boldsymbol{R}_{65}$ at both ends were determined using the Timoshenko beam model.

**Table 3. Three different overhang lengths of the tool shank**

| Case | Length | | |
|---|---|---|---|
| | $l_s$/mm | $l_i$/mm | $l_b$/mm |
| 1 | 13.30 | 38.10 | 6.79 |
| 2 | 19.65 | 31.75 | 13.14 |
| 3 | 26.00 | 25.40 | 19.49 |

Fig. 7 shows the receptances $\boldsymbol{h}_{55}$ of the three different overhang lengths of tool shank for the frequency range from 200 Hz to 2 000 Hz; the three cases described in Table 3 are presented. Similar to the fluted portion, no resonance occurred in this range; small numerical noise is observed below 600 Hz in the imaginary part of the response.

## 4 Receptance Coupling of Components with Spindle-machine

### 4.1 Receptance of the spindle-machine

Compared to the holder and tool shank, the receptance of spindle-machine is more difficult to model. Spindle dynamics modeling, often completed by FEM, requires detailed information on its structural design, bearing stiffness values and damping levels. Such knowledge, however, is generally unavailable for the end user. Therefore, impact testing is used in the RCSA approach to determine the required receptances. First, a standard artifact with a simple cylindrical geometry is inserted in the spindle and direct and cross receptances are recorded by impact testing. Second, the portion of standard artifact beyond the flange is removed in simulation (inverse RCSA) to isolate the spindle-machine response.

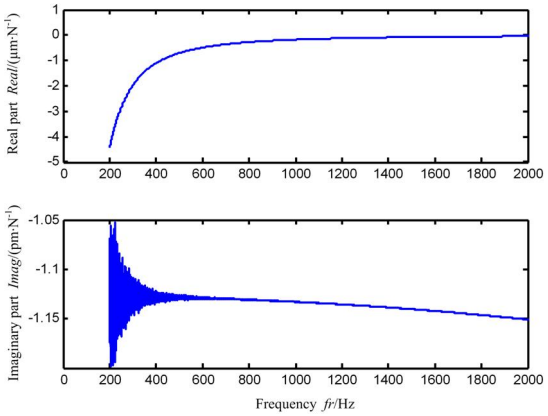


(a) Case 1

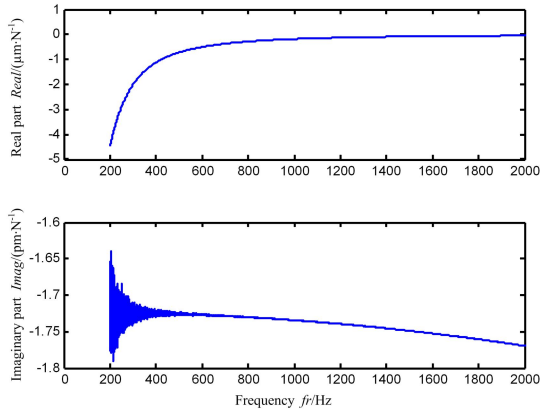


(b) Case 2

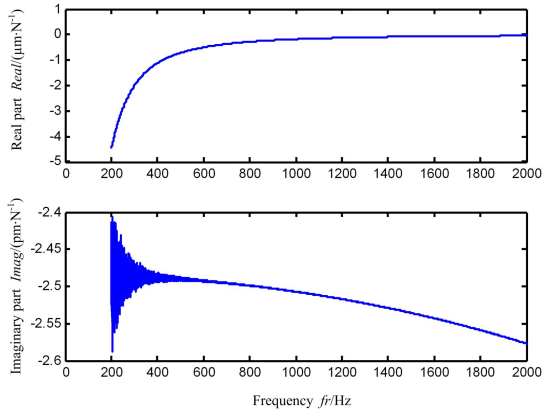


(c) Case 3

Fig. 7. Predicted receptance $\boldsymbol{h}_{55}$ of the tool shank and holder

Measurements were performed on a Mikron UCP 600 Vario milling machine equipped with a Step-Tec 20 kr/min, 16 kW cartridge-type spindle. A standard artifact was clamped in the spindle (HSK-63A interface). A low mass accelerometer was used to record the vibration response to an impact applied using a PCB 086B03 impact hammer. A MLI MetalMax 6.0 data acquisition system was used for data collection.

### 4.2 Components receptance coupling

The component receptances are coupled using RCSA. Two models were evaluated: 1) the actual fluted portion receptances ($\boldsymbol{R}_{11}$ and $\boldsymbol{R}_{22}$) were coupled with the tool shank-holder receptances ($\boldsymbol{R}_{55}$ and $\boldsymbol{R}_{66}$) and then the spindle-machine receptances ($\boldsymbol{R}_{77}$), which is abbreviated to AF model; and 2) the equivalent diameter beam receptances ($\boldsymbol{R}_{33}$ and $\boldsymbol{R}_{44}$) were coupled with the tool shank-holder receptances ($\boldsymbol{R}_{55}$ and $\boldsymbol{R}_{66}$) and then the spindle-machine receptances ($\boldsymbol{R}_{77}$), which is abbreviated to EDB model.

Three cases with different tool overhang lengths were evaluated; the associated assembly (machine-spindle-holder-tool) receptances $\boldsymbol{H}$ are shown in Fig. 8. From these tool point receptance plots, it can be seen that the prediction accuracies of the two models are acceptable. The results are summarized in Table 4.

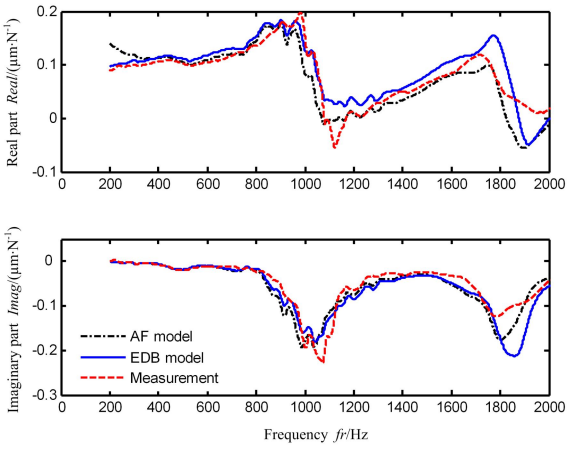


(a) Case 1

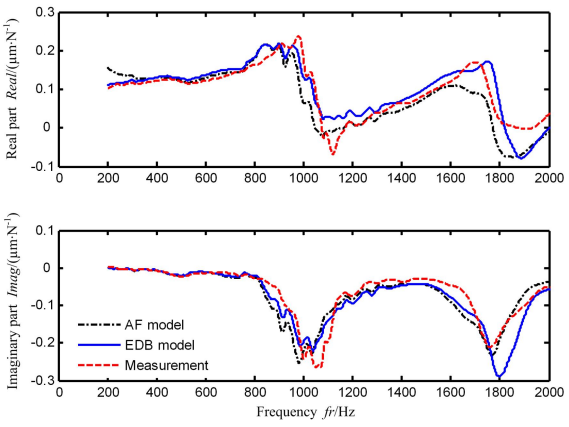


(b) Case 2

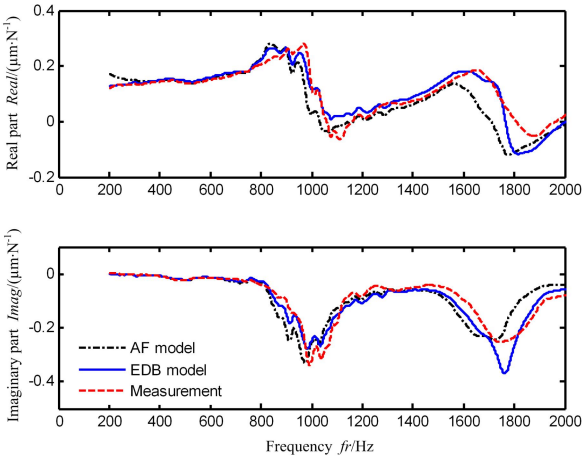


(c) Case 3

Fig. 8. Associated assembly (machine-spindle- holder-tool) receptances $\boldsymbol{H}$

**Table 4. Natural frequency predicted by AF and EDB model** Hz

| Case | Mode | Experiment | AF model | EDB model |
|---|---|---|---|---|
| 1 | 1st | 1 072 | 1 038 (3.17%) | 1 042 (2.80%) |
| | 2nd | 1 785 | 1 806 (1.18%) | 1 860 (4.20%) |
| 2 | 1st | 1 050 | 1 033 (1.62%) | 1 037 (1.24%) |
| | 2nd | 1 762 | 1 769 (0.40%) | 1 800 (2.16%) |
| 3 | 1st | 992 | 976 (1.61%) | 984 (0.81%) |
| | 2nd | 1 740 | 1 730 (0.58%) | 1 761 (1.21%) |

## 5 Conclusions

The predictions of assembly dynamics for machine-spindle-holder-fluted tool assemblies were completed using the RCSA technique. The receptances for the fluted portion of the tool were calculated by FEM and an equivalent beam diameter Timoshenko model. The tool shank and holder receptances were also modeled using Timoshenko beam theory, while the machine-spindle receptances was measured by impact testing. The following conclusions can be drawn from this study:

(1) FEM can be successfully used for the receptance prediction of the fluted portion.

(2) Through comparison with the FEM solution of the fluted portion, it was shown that the equivalent diameter Timoshenko beam model is an acceptable approximation.

(3) From the coupling results of the AF and EDB models for three cases of tool overhang lengths, both model predictions showed good agreement with experiment, the errors are all less than 5%.

### References

[1] TLUSTY J. Dynamics of high-speed milling[J]. *Transactions of ASME Journal of Engineering for Industry*, 1984, 108(2): 59–67.

[2] SMITH S, TLUSTY J. Update on high-speed milling dynamics[J]. *Transactions of the ASME Journal of Engineering for Industry*, 1990, 112(2): 142–149.

[3] ALTINTAS Y, BUDAK E. Analytical prediction of stability lobes in milling[J]. *Annals of the CIRP*, 1995, 44(1): 357–362.

[4] SCHMITZ T, DONALDSON R. Predicting high-speed machining dynamics by substructure analysis[J]. *Annals of the CIRP*, 2000, 49(1): 303–308.

[5] SCHMITZ T, DAVIES M, KENNEDY M. Tool point frequency response prediction for high-speed machining by RCSA[J]. *Journal of Manufacturing Science and Engineering*, 2001, 123(4): 700–707.
[6] SCHMITZ T, DAVIES M, MEDICUS K, et al. Improving high-speed machining material removal rates by rapid dynamic analysis[J]. *Annals of the CIRP*, 2001, 50(1): 263–268.
[7] SCHMITZ T, POWELL K, WON D, et al. Shrink fit tool holder connection stiffness/damping modeling for frequency response prediction in milling[J]. *International Journal of Machine Tools and Manufacture*, 2007, 47(9): 1 368–1 380.
[8] PARK S S, ALTINTAS Y, MOVAHHEDY M. Receptance coupling for end mills[J]. *International Journal of Machine Tools and Manufacture*, 2003, 43(9): 889–896.
[9] ERTÜRK A, ÖZGÜVEN H N, BUDAK E. Analytical modeling of spindle-tool dynamics on machine tools using Timoshenko beam model and receptance coupling for the prediction of tool point FRF[J]. *International Journal of Machine Tools and Manufacture* 2006, 46: 1 901–1 912.
[10] NAMAZI M, ALTINTAS Y, ABE T, et al. Modeling and identification of tool holder-spindle interface dynamics[J]. *International Journal of Machine Tools & Manufacture*, 2007, 47(9): 1 333–1 341.
[11] FILIZ S, CHENG C H, Powell K B, et al. An improved tool-holder model for RCSA tool-point frequency response prediction[J]. *Precision Engineering*, 2009, 33(1): 26–36.
[12] KOPS L, VO D. Determination of the equivalent diameter of an end mill based on its compliance[J]. *Annals of the CIRP*, 1990, 39(1): 93–96.
[13] KIVANC E, BUDAK E. Structural modeling of end mills for form error and stability analysis[J]. *International Journal of Machine Tools and Manufacture*, 2004, 44(11): 1 151–1 161.
[14] WEAVER J W, TIMOSHENKO P, YOUNG D. *Vibration problems in engineering*[M]. New York: John Wiley and Sons, 1990.
[15] YOKOYAMA T. Vibrations of a hanging Timoshenko beam under gravity[J]. *Journal of Sound and Vibration*, 1990, 141(2): 245–258.

## Biographical notes

ZHANG Jun, born in 1978, is currently a lecturer in *State Key Laboratory for Manufacturing System Engineering, Xi'an Jiaotong University, China*. He was a joint PhD candidate in *Xi'an Jiaotong University, China*, and *University of Florida, USA*, and received his PhD degree from *Xi'an Jiaotong University, China*, in 2009. His research interest includes high-speed machining.
Tel: +86-29-83399529; E-mail: junzhang@mail.xjtu.edu.cn

SCHMITZ Tony, born in 1970, is currently an associate professor in *Department of Mechanical and Aerospace Engineering, University of Florida, USA*. His research interests include high-speed machining, sensor development and accuracy evaluation.
Tel: +1-352-3920961; E-mail: tschmitz@ufl.edu

ZHAO Wanhua, born in 1965, is currently a professor and a PhD candidate supervisor in *State Key Laboratory for Manufacturing System Engineering, Xi'an Jiaotong University, China*.
Tel: +86-29-83399520; E-mail: whzhao@mail.xjtu.edu.cn

LU Bingheng, born in 1945, is currently an academician in *Chinese Academy of Engineering, China*, and a professor in *Xi'an Jiaotong University, China*.
E-mail: bhlu@mail.xjtu.edu.cn